Alex DECKMYN, Daan DEGRAUWE, Luc GERARD, Rafiq HAMDI,
Geert SMET, Piet TERMONIA
Royal Meteorological Institute, Brussels, Belgium

The operational ALADIN-Belgium model

1. Main features

- Model version: AL35t1 + ALARO-0 + 3MT
- 60 hour production forecasts four times a day (0, 6, 12 and 18 UTC).
- Lateral boundary conditions from ALADIN-France and Arpege global model.

2. The computer system

- SGI Altix 4700.
- 196 Itanium2 CPUs

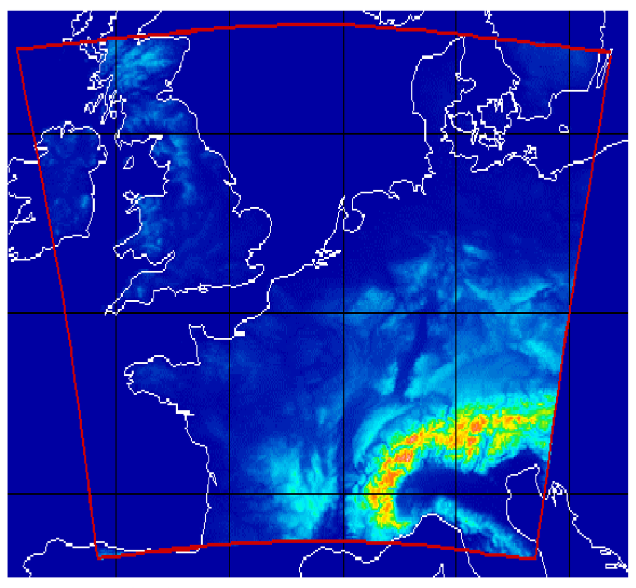

3. Model geometry

- 7 km horizontal resolution (240*240 points).
- 4 km resolution (192*192)
- 46 vertical levels
- Linear spectral truncation.
- Lambert projection.

4. Forecast settings

- Digital filter initialization (DFI with LSPRT=.FALSE.).
- two time level semi-implicit semi-Lagrangian - SISL - advection scheme.
- Time step: 300s (7 km), 180s (4 km)
- Lateral boundary condition coupling at every 3 hours.
- Hourly post-processing (latitude-longitude and Lambert).

5. Operational suite/technical aspects

- Transfer of coupling file from Météo-France via Internet (primary channel) and the Regional Meteorological Data Communication Network (RMDCN, backup).
- Model integration on 40 processors (7 km), 20 processors (4 km).
- Post-processing on 8*1 processors.
- Continuous monitoring supported by a home-made Kornshell/Web interface.
- Monitoring with SMS (Supervisor Monitor Scheduler).

Complex Wavelet representation of background error covariances

A new representation of background error covariances has been implemented in the ALADIN 3d-Var code. In the current operational code, the covariance matrix B is represented as a block-diagonal matrix in spectral space. As a result, the structure functions are homogeneous and isotropic over the whole domain.

With increasing resolution, the importance of heterogeneous (location-dependent) and anisotropic structure functions is however growing.

An experimental representation using *Dual Tree Complex Wavelets* (Kingsbury 1999) has now been added to the ALADIN code. In wavelet space, a diagonal B matrix can still represent some local differentiation. In addition, the phase difference between the real and imaginary part in vertical covariances, allows us to model tilted structure functions.'

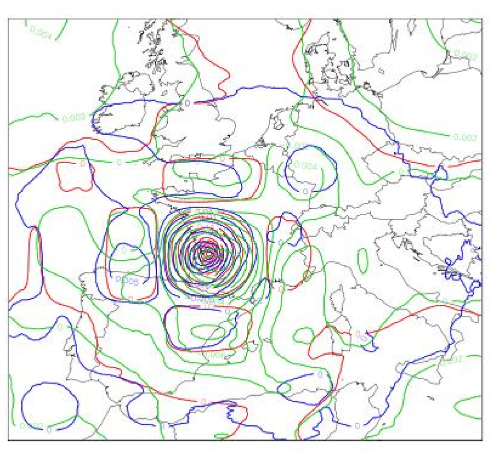

Analysis increments (T) for a temperature observation at 500Hpa.

Red: at 500Hpa

Blue: lowest model level

Green: high atmosphere

Notice that they are not centered: there is a slight tilt to the structure function.

Precipitation verification with SAL

SAL (Wernli et al., 2008) is a novel verification method to compare model-predicted precipitation with observations from raingauge data or radar imagery. It expresses the quality of a forecast by means of three components: Structure, Amplitude and Location.

S : -2 (predicted structures too small) -> 2 (predicted structures too large)

A : -2 (predicted amount too small) -> 2 (predicted amount too large)

L : 0 (correct predicted location) -> 2 (wrong location)

SAL was implemented at RMI and used to compare the precipitation forecast of ALADIN (7km) with ALARO (4km). The figures show the scores of these to models over Belgium in May 2009. The observed precipitation fields were extracted from radar data. Grey data points indicate days with low precipitation (<1mm). It appears that the higher resolution model ALARO provides a more accurate forecast than ALADIN: the scatter on the Structure component is reduced; the bias on the Amplitude component almost completely disappears; and also regarding the Location component, ALARO performs slightly better than ALADIN. A significant positive bias remains, however, on the Structure component, which indicates that the predicted precipitation structures are too large.

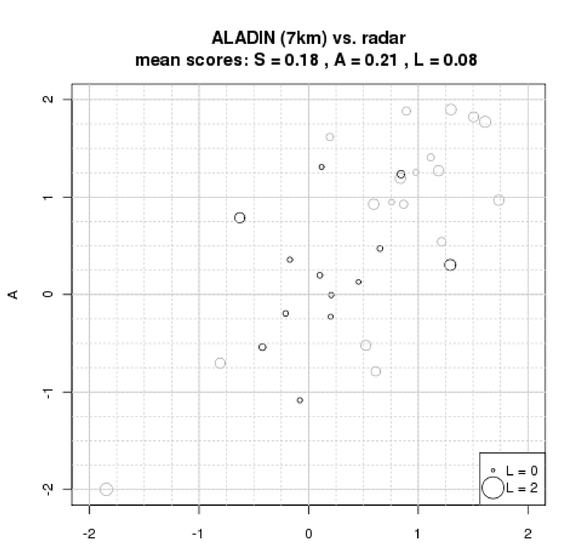

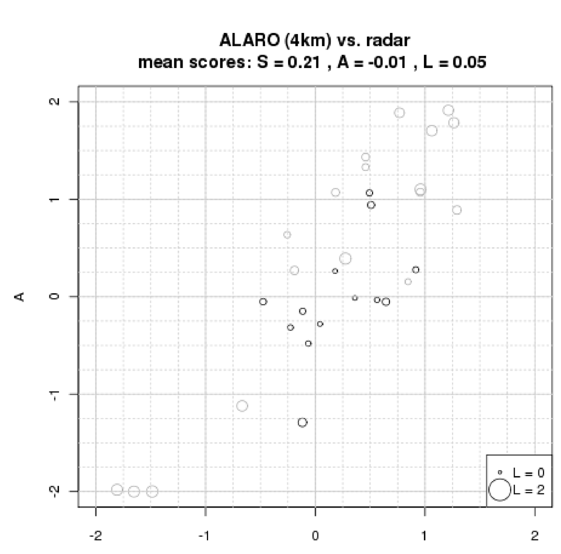

Work on the improvement of the deep convection parameterization in high resolution limit (3MT for Alaro-1).

To behave satisfyingly at high resolution (below 8km), the deep convection parameterization has to account for the time-evolution of the updraft vertical velocity, of the updraft horizontal extents and of its vertical extent (gradual raise of the cloud, while no steady-state is reached), and must prevent concurrence between resolved and subgrid.

In the point of view of modeling, the two first items can be handled by memorizing respectively an updraft velocity variable governed by a prognostic equation, and an updraft mesh fraction evolving at each time step. Both variables are advected by the mean flow.

This technique was applied in the 3MT scheme [Gerard et al., 2009], together with a sequential organization of the parameterizations to make them complementary (e.g. preventing concurrence on a same source of moisture). The updraft condensation was combined with the resolved condensation before entering a single microphysics. Special attention was given in the interaction of the parametrizations within the time-step and between time-steps.

This 'Alaro-0 solution' appears quite satisfactory down to 4km resolution, but the auto-extinction of the parameterization at higher resolution is not realised.

To go further, we developed a new scheme based on the concept of 'virtual unresolved updraft'.

It considers that physical updrafts can already be partly represented by the resolved motion and the resolved condensation scheme, and that parameterization should simply produce a complementary contribution to these.

The virtual updraft is necessarily confined in a grid column. An upwards motion of the updraft parcel (wrt the mean grid-box motion) is compensated by a downwards motion of the dryer environment.
Following e.g. Asai and Kasahara [1967], the subsiding motion is accompanied by a dry adiabatic heating reducing the net buoyancy. This effect is accounted for in our formulation, and depending of the vertical dry and moist lapse rates, the maximum consumption of energy by the subgrid updraft occurs for a mesh fraction of at most 0.4, which is also the largest possible value for it.

The short time-steps make it necessary to allow a gradual rise of the updraft top; the vertical equation also accounts for the fraction of the time-step a given level is reached by the rising updraft. The mesh-fraction evolution is currently estimated with a diagnostic of the steady-state value (not reached) and an evolution equation towards it.
Preliminary tests at varying resolution in three-dimensional model show a significant decrease – though not a complete extinction – of the convective contribution when the mesh-size decreases from 8 to 1km (see figure).

Our further developments also include the use of a CAPE closure, together with a triggering based on a TKE threshold.

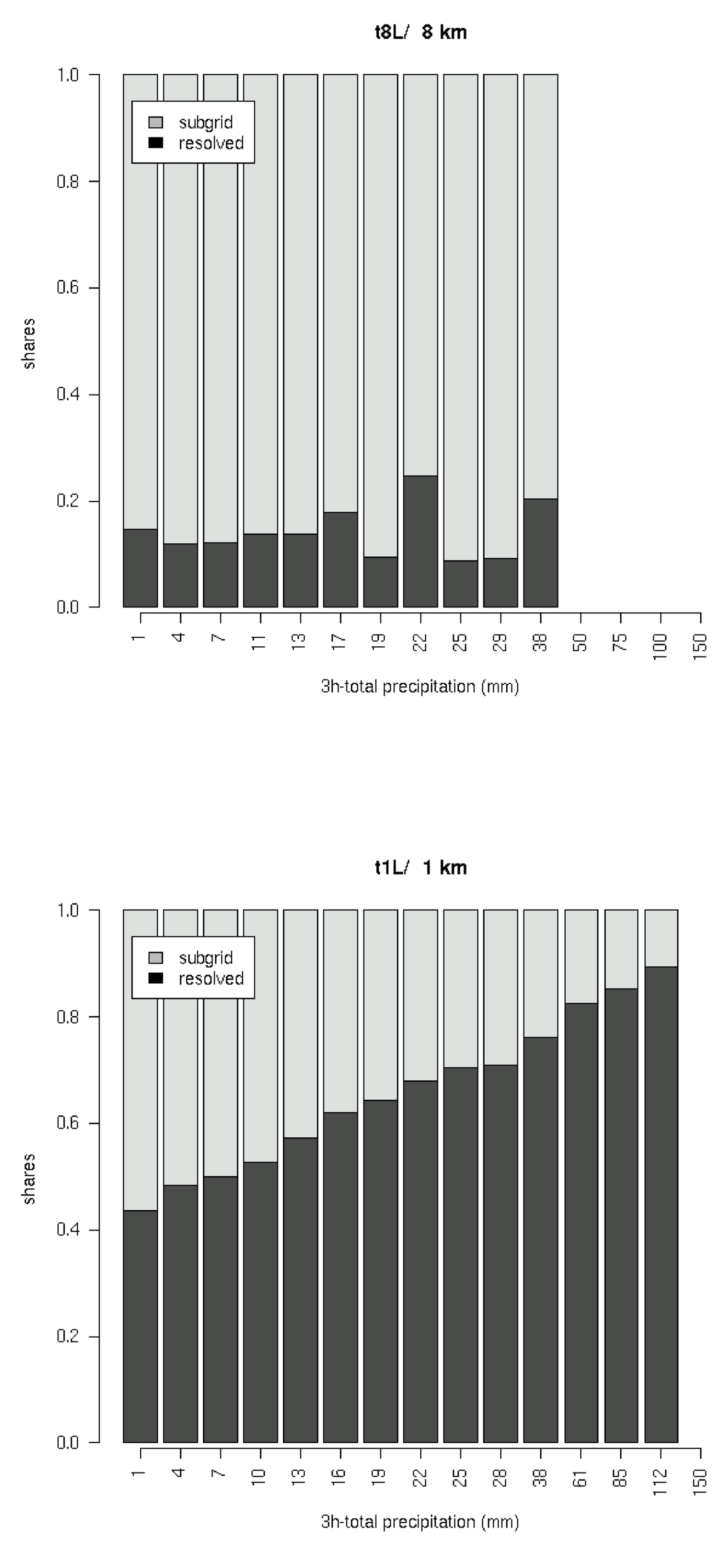

Figure 1 : Resolved and subgrid respective proportions for several classes of forecast surface precipitation intensities. Convective event over Belgium (10-09-2005). top: 1km-, bottom: 1km-mesh-size

Development of an academic NWP model: CHAPEAU

To improve the collaboration between the academic world and the NWP community, a model version is required that focuses on accessibility rather than on efficiency. To this goal, KNMI and RMI have taken the first steps towards the development of CHAPEAU (Common Harmonie and Aladin Package for Educational and other Academic Use).

The main purposes of CHAPEAU are:
- use as an educational tool for meteorology students
- facilitate research at universities on a fully functional NWP model
- allow for this research to find its way back to operational models

Characteristics of CHAPEAU are:
- standalone package, easy to install
- works on a regular Linux-PC
- easy post-processing

Effects of historical urbanization in the Brussels Capital Region on surface air temperature time series: a model study

In this study we updated previous research on the Brussels Capital Region (BCR) by analyzing the local impact of change in impervious surfaces on long-term trends in mean and extreme temperatures between 1960 and 1999. Specifically, we combine data from remote sensing imagery and the newly developed surface scheme of Météo-France SURFEX (SURFace Externalisée) including the multi-layer version of the Town Energy Balance (TEB) (see Hamdi and Masson (2008) for more details). In the present study: (i) we use SURFEX in a stand-alone mode, coupled to downscaled ERA-40 reanalysis data, (ii) we consider BCR as a lumped urban volume.

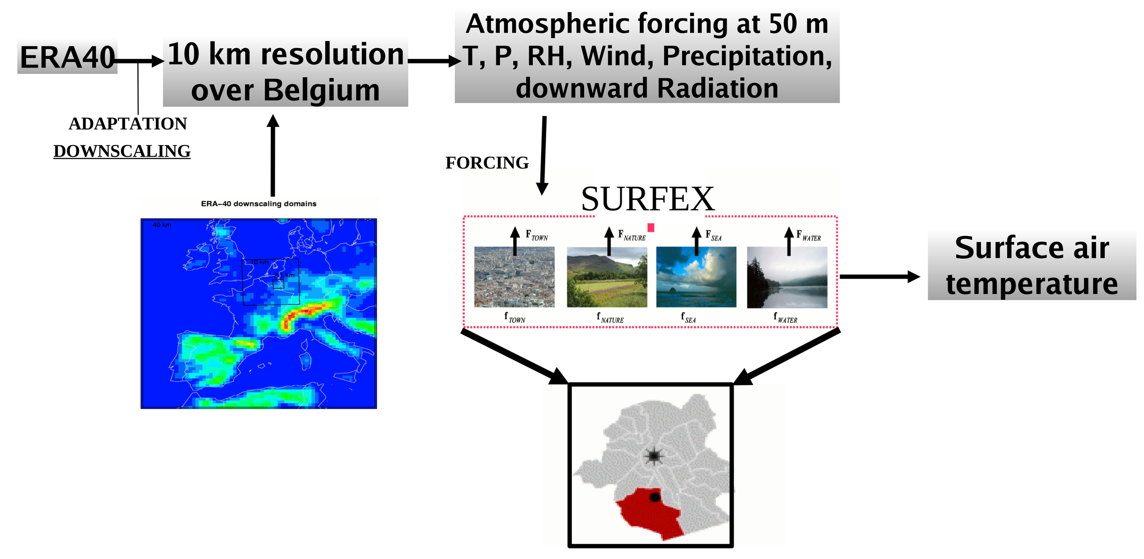

To isolate effects of urbanization on local near surface climate conditions, we performed model simulations according to two scenarios, which correspond to different states of urbanization:

(i) the "rural" scenario represented a hypothetical situation with no urban areas inside the domain during the 40 years. Radiative and thermal properties of the vegetation cover (albedo, roughness length, emissivity, thermal inertia, leaf area index, etc.) are taken from the ECOCLIMAP database (Masson et al., 2003) and remained fixed through the simulation.

(ii) the "urban" scenario represented the climate in the presence of urban areas using the evolution of surface cover fractions. For this run, the surface cover fractions are updated each year using a linear interpolation. In this study, geometrical, thermal, and radiative properties of roofs, walls, and roads were averaged over available data (Hamdi and Masson, 2008, Trusilova et al., 2008) and were set to values representing a typical midsize European city.

Estimation of urban bias on the annual trend

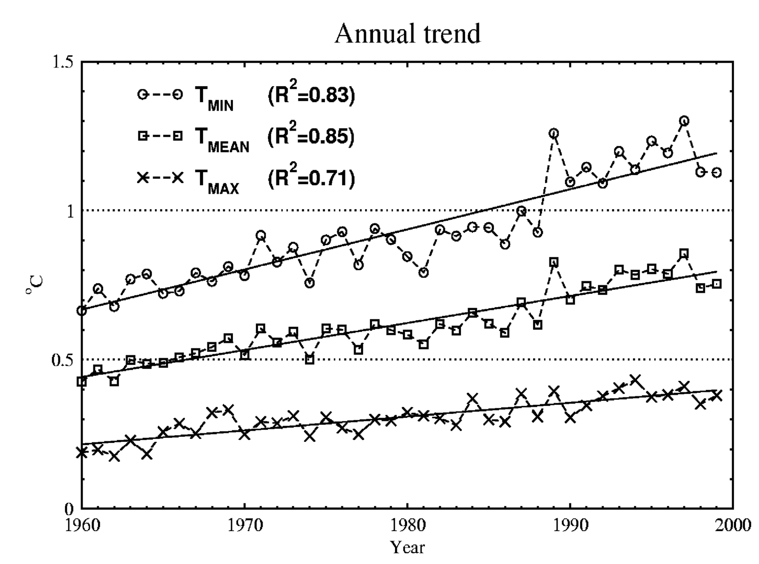

As indicated by the spacing between the curves, annual mean urban bias (AMUB) on minimum temperature is shown to be rising at a higher rate (slightly 3 times) than on maximum temperature, with a linear trend of 0.14°C and 0.05°C per decade respectively.

Using the AMUB on mean temperatures, we now estimate that 45% (ratio between the linear trend of the AMUB and the urban scenario) of the overall warming trend is attributed to intensifying urban heat island effects rather than to changes in local/regional climate. This should correspond to ~0.63 °C of the 20th century warming trend of 1.4 °C in the Uccle series.

References:

Geleyn J.-F., B. Catry, Y. Bouteloup and R. Brožkova, 2008: A statistical approach for sedimentation inside a micro-physical precipitation scheme. *Tellus* 60A, pp 649-662

L. Gerard, J.-M. Piriou, R. Brozkova, J.-F. Geleyn, and D. Banciu. Cloud and precipitation parameterization in a meso-gamma scale operational weather prediction model. *Mon.Wea.Rev*, 137:3960–3977, 2009.

Gerard L. 2007: An integrated package for subgrid convection, clouds and precipitation compatible with meso-gamma scales. *Q. J. R. Meteorol. Soc.* 133, pp 711-730.

Piriou J.-M., J.-L. Redelsperger, J.-F. Geleyn, J.-P. Lafore and F. Guichard, 2007: An approach for convective parameterization with memory, in separating microphysics and transport in grid-scale equations. *J. Atmos. Sci.* 64, pp 4127-4139.

Vána F., 2006: General introduction and description of the SLHD : Semi-Lagrangian Horizontal Diffusion (March 2006) (Dynamics). Aladin/Alaro-0 internal documentation.

Hamdi, R., and V. Masson, 2008: Inclusion of a drag approach in the Town Energy Balance (TEB) scheme: offline 1-D evaluation in a street canyon. *J. Appl. Meteor. Clim.*, **47**, 2627-2644.

Masson, V., J.-L. Champeaux, F. Chauvin, C. Meriguet, and R. Lacaze, 2003: A global database of land surface parameters at 1km resolution in meteorological and climate models. *J. Climate*, **16**, 1261-1282.

Trusilova K., M. Jung, G. Churkina, U. Karstens, M. Heimann, and M. Claussen, 2008: Urbanization impact on the climate in Europe: Numerical experiments by the PSU-NCAR mesoscale model (MM5). *J. Appl. Meteor. Clim.*, 47, 1442-1455.